Eos, Vol. 75, No. 27, July 5, 1994

EOS, TRANSACTIONS, AMERICAN GEOPHYSICAL UNION

EOS

VOLUME 75 NUMBER 27

JULY 5, 1994

PAGES 305-312

Watching for Fireballs on Jupiter

PAGES 305, 307, 310

Mark B. Boslough, David A. Crawford, Allen C. Robinson, and Timothy G. Trucano

Over a period spanning six nights starting July 16, a series of hypervelocity impacts will take place on a scale never before witnessed. Comet fragments of sizes possibly measured in kilometers will collide with Jupiter at 60 km/s.

This event has captured the imaginations of planetary scientists, professional and amateur astronomers, physicists, seismologists, atmospheric scientists, theoretical astrophysicists, and computational mathematicians. Current expectations are that the fragments of Comet Shoemaker-Levy 9 will be too small to generate impacts that will be visible to Earth-based observers.

However, fragments with diameters greater than a kilometer have not been ruled out. Such fragments would generate giant fireballs that would be observable from Earth within a minute of impact time for at least some of the events. Moreover, careful measurement of the times that these fireballs appear would allow good estimates of the comet fragment masses. An impact-produced fireball would consist of very hot (>2000 K) mixed atmospheric and cometary material moving upward supersonically, driving a shock wave ahead of it.

Our purpose for modeling the first 100 s of such an impact is twofold. First, we hope the impacts will provide a means to validate our shock physics codes, CTH and PCTH, [*McGlaun et al.*, 1990] at velocity, size, and energy scales many orders of magnitude greater than we can attain in the laboratory. Second, we wish to provide predictions that will guide astronomical observations and help interpret the data.

What phenomena will be observable in the first few minutes after impact? And what information can be derived from these observations?

Our simulations show that if the largest fragments are indeed greater than 1 km in diameter, then at least some of the impacts should generate fireballs that are directly visible from the Earth within a minute after impact. In addition, these fireballs consist of adiabatically expanding and cooling debris clouds launched into ballistic trajectories that put them in direct sunlight within another minute or two.

The observational timing of these two events—arrival of the fireball over Jupiter's limb, and its subsequent emergence into the sunlight—would define the trajectory of the fireball/debris cloud and provide data sufficient to determine the actual sizes of the impacting fragments. The possibility of making these useful observations is a direct result of the fortuitous arrangement of the Earth and Sun with respect to the points of impact, just beyond Jupiter's limb (horizon) as viewed from Earth. In another paper [*Boslough et al.*, 1994], we suggested that it may be possible to detect two distinct arrivals over the limb: first, the shock wave and, a few seconds later, the fireball.

Impacts of Shoemaker-Levy 9

When the trajectories of the twenty-odd large fragments of comet Shoemaker-Levy 9 were refined by better astrometric data early this year, it became apparent that the points of impact were not deep on the back side as originally thought, but were tantalizingly close to Jupiter's horizon. In fact, as of June 23, the predictions of P. W. Chodas and D. K. Yeomans indicate that the final fragment "W" will hit Jupiter barely less than 4° beyond the southwest limb of the planet. These newer impact locations encouraged us to focus our attention on the aspects of the impacts that would potentially be observable from Earth.

The results of our simulations have exceeded our expectations. In the best case scenario, with the largest fragments ranging from 2–4 km in diameter, the impact-produced fireballs will be bright enough to be seen next to the sunlit surface of Jupiter for the first moments as they rise above Jupiter's limb. In a less optimistic, but probably more realistic picture, the largest fragments, are only about 1 km in diameter. In this case, the fireballs would be significantly dimmer, and may be close to the visibility threshold for the fragments that hit closest to the limb. In the most pessimistic view, there is almost no mass to the fragments. If this proves to be true, then there will be no observable fireball or debris from any of the impacts. Unfortunately, the actual fragment sizes cannot be determined from telescope images and will not be known until they hit Jupiter.

Computational Simulations

With the impending series of impacts, nature has provided our group with an unprecedented means of testing our shock physics simulation capabilities with Sandia's 1840-node Intel Paragon, currently the world's most powerful parallel computer. We have taken advantage of this unique capability to run the first high-resolution (3-km and

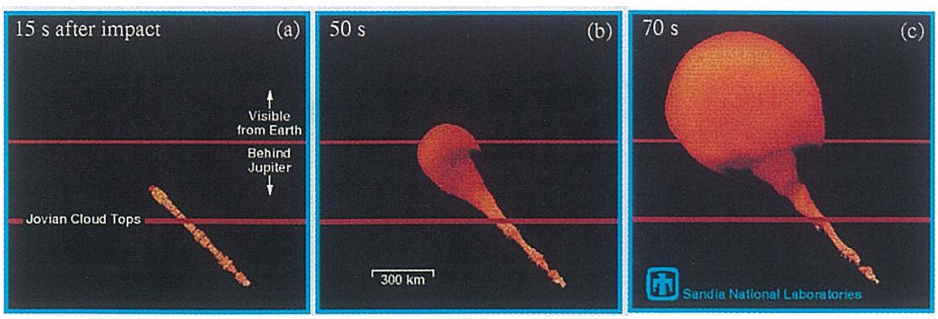

Fig. 1. Fireball generated by 3-km diameter ice fragment; (a) about 15 s after impact; (b) growing at 50 s, with spherical shock wave forming; (c) at 70 s, with expanding spherical shock. These massively parallel three-dimensional simulations were performed on Sandia's 1840-node Intel Paragon, currently the world's fastest supercomputer. Original color image appears at the back of this volume.

Sandia National Laboratories, Albuquerque, NM 87185-0821

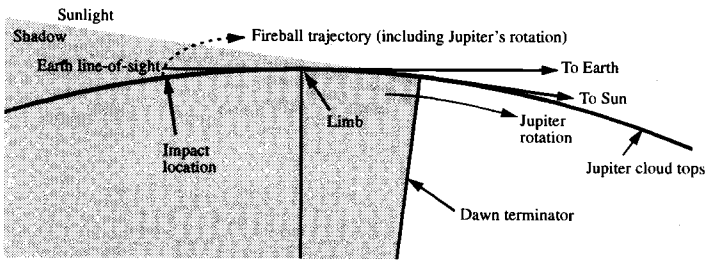

Fig. 2. Lateral view of the impact geometry. Ballistic fireball/debris trajectory crosses into line-of-sight from Earth and then into sunlight.

5-km zone) three-dimensional simulations of the immediate after-effects of impact: the development and growth of the fireball. A large number of computational elements—up to 8 million zones—is required for these simulations to contain the large extent of the fireball after a minute or so, while still retaining features on a small spatial scale. In addition, an oblique impact is an inherently three-dimensional problem, and a realistic simulation must treat it as such. These are the only high-resolution, three-dimensional fireball simulations to date, and we believe they are sufficiently reliable to provide the basis for our predictions.

To provide an input for the fireball simulations, we first ran a series of two-dimensional axisymmetric simulations of the entry, penetration, and breakup of the cometary fragments. Two-dimensional simulations were required at the beginning to provide the much higher resolution needed to simulate the details of the comet entry. This phase of the simulation made use of the CTH Eulerian shock-physics code, run in a "reverse ballistic" reference frame in which the Jovian atmosphere was propelled upward at 60 km/s into the cometary fragment. The Eulerian mesh was extended above the comet fragment for 1000 km to preserve materials and to state variables and velocity fields for insertion into the three-dimensional fireball simulation.

We assumed that the fragment was composed of water ice at full density and an initial temperature of 100 K. An ANEOS table [*Thompson*, 1989], which includes thermal expansion, melting, and vaporization, provided the equation of state for the ice. The equation of state for the Jovian atmosphere was constructed by G. I. Kerley, and represents a hydrogen-helium mixture that can undergo both dissociation and ionization.

We performed a series of two-dimensional simulations with comet fragments of various sizes, shapes, and strengths. The most important determining factor for the depth of penetration of the fragment is its total mass, given reasonable values for the other parameters that we varied. The mean penetration depths for 1, 2, and 3 km diameter ice spheres were about 150, 240, and 280 km beneath the 1 bar level, respectively.

Other workers have predicted somewhat different penetration depths. For example, K. Zahnle and MacLow predict less penetration. However, they have used a gas equation of state for their cometary fragment, which causes it to expand to a lower density at the beginning of the simulation. *Takata et al.* [1994] have used smoothed particle hydrodynamics simulations to predict slightly deeper penetrations.

As the comet fragments penetrate the atmosphere, they lose mass and kinetic energy along their trajectory. The Eulerian grid stores spatially resolved density, temperature, fluid velocity, and pressure distributions resulting from this hypervelocity interaction. By spatially averaging these fields, rotating them 45°, and inserting them into a three-dimensional mesh, the scaled two-dimensional simulations provided initial conditions for our three dimensional fireball simulations. The two-dimensional symmetry is broken when the fireball begins to grow because it is influenced by the inclined atmospheric density gradient, so three-dimensional simulations are required. Sandia's Intel Paragon, an 1840-processor massively parallel supercomputer, was used for the fireball simulations with PCTH, a parallel version of the CTH Eulerian shock physics code. These simulations determine the evolution and growth of fireballs during a period of up to 100 s after the impact of 1-km and 3-km diameter ice spheres. The simulations are described in more detail by *Crawford et al.* [1994].

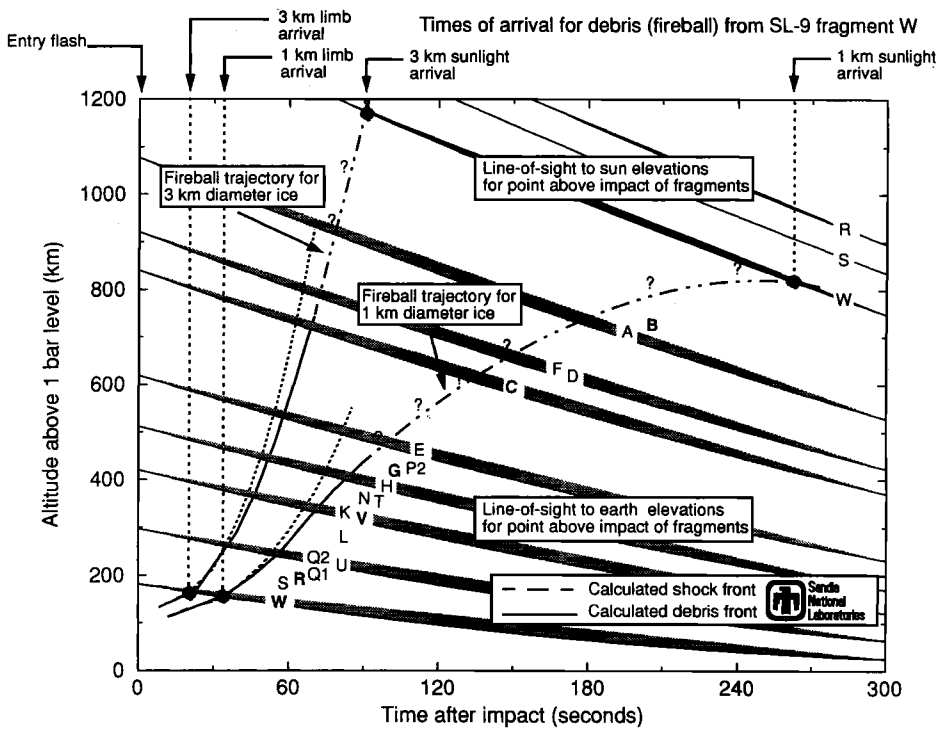

Fig. 3. Calculated trajectories of shock wave and debris front (fireball) from three-dimensional CTH simulations for 1- and 3-km diameter ice fragments. Approximate line-of-sight elevations to Earth (light shading) and to the Sun (dark shading) are based on the impact locations for the fragments (identified by letters) calculated by Chodas and Yeomans as of June 23, assuming the Jovian limb is defined by the cloud tops, and ignoring refraction. They allow potentially observable arrival times to be estimated. Boldface letters identify fragments that will have impacts that may be observable from U.S. locations, with (C,G,R, and W) from Hawaii, (B,C,R, and V) from parts of the western states, and (B and V) from parts of the eastern states.

Ballistic Fireballs: Observable for Big Impacts

The result of our fireball simulation for a 3-km fragment impact is depicted in Figure 1. The fireball and surrounding shock wave are shown about 15, 50, and 70 s after impact. At 15 s, the comet has penetrated to its maximum depth, well below the outermost visible cloud tops of Jupiter's atmosphere, leaving behind it a trail of hot, high-pressure air and cometary debris, which expands explosively into the surrounding atmosphere. This creates a fireball that grows supersonically upward, initially along the entry path. After 50 s, a spherical shock wave can be seen separating from the fireball. It is accelerating upward at 10 km/s and has reached a diame-

ter of 300 km and an altitude of 450 km above the Jovian cloud tops. At 70 s, the spherical shock wave is advancing upward at a velocity of 25 km/s. It has reached a diameter of 700 km and an altitude of 900 km above the clouds.

For reference, the locations of the cloud tops and the limb of Jupiter (as seen from Earth) are shown. The limb position assumes that the impact occurred 6 beyond the limb, and that the cloud tops form the visible limb. If the effective limb is determined by high stratospheric hazes, it could be as much as 35-40 km higher. This would delay the line-of-sight arrivals by a few seconds. As of June 23, the Chodas and Yeomans estimates of impact locations range from about 4-10°beyond the limb.

Hidden within the spherical shock wave in Figure 1 is the fireball itself, which is a rapidly rising cloud of cometary debris and Jovian atmosphere at very high temperature (at 70 s, the fireball is still at 1700 K, and the shock wave is 2300 K). Because the fireball contains much of the cometary material, we believe it will be optically thick and radiating at this temperature. If this is true, its apparent bolometric magnitude (as viewed from Earth) would be about 2 (luminosity = 4 x 1023 erg/s, λ_{max} = 1.7 μm) at this time. This estimate assumes the following: The light is from the visible part of a fireball generated by a 3-km diameter icy impactor 70 s after impact, the impact location is 6° beyond the limb, the fireball is optically thick with cometary debris, and there is no contribution from the high-temperature shock wave. An apparent magnitude of 2 is about 25 times brighter than the Galilean satellites, but only about one-fiftieth as bright as Jupiter itself. The bolometric flux (surface brightness) of the fireball is thousands of times greater than that of sunlight reflected from Jupiter (per unit surface area), but the source is much smaller (with radiating area less than 1% of the reflecting area of the Galilean satellites). Impacts close to the limb will reveal more of the fireball for a brighter magnitude (a 3-km impact 4° beyond the limb yields L = 10^{24} ergs/s, λ_{max} = 1.2 μm). Small, 1-km impactors far from the limb will probably not be visible, whereas those close to the limb will yield dim fireballs (L = 1021–1022 ergs/s, λ_{max} = 1.3–1.5 μm). Because the visible fireballs will be orange, fading to red and disappearing over the course of seconds to minutes (depending on impactor size), the application of a red or orange filter will optimize contrast for visual observations; however, most of the energy will be radiated in the near infrared.

We are calling this very hot debris cloud a fireball, but the differences between it and other closely related phenomena should be outlined. Analogies to the fireball associated with the detonation of a nuclear device are limited. The development of a nuclear fireball is dominated by interior radiative transport at temperatures of tens of millions of degrees. Some fraction of this energy forms a shock wave in the atmosphere, which separates from the fireball but can still be luminous if strong enough. The shock wave generated by the impact fireball is similar to the outer, mechanically driven nuclear blast wave, but the temperature of the impact-generated shock wave is higher at a given propagation distance because the energy source is about six orders of magnitude greater than a megaton-scale nuclear device.

The fireball itself is a ballistically rising (as opposed to buoyant) mixture of shocked atmosphere and vaporized cometary material. A nuclear fireball that is small compared to the scale height of the atmosphere will be driven upward by buoyant forces because it is less dense than the surrounding atmosphere. A large impact fireball will be much greater than the scale height of the Jovian atmosphere. The atmospheric pressure is much greater at the bottom than at the top, so it will accelerate upwards as if shot from a gun, even though its density is much greater than the surrounding atmosphere at the top. Its inertia will carry it on a ballistic trajectory, which rises to more than 1000 km above the clouds.

It should also be pointed out that at 70 s in Figure 1, the fireball and spherical shock appear to be mushroom shaped. This should not be misconstrued as a mushroom cloud, which is due to toroidal circulation of hot gasses and condensation associated with a buoyantly rising fireball and happens long after the shock wave has passed. The reason for a similar appearance in the rendering of Figure 1 is because the shock wave is primarily directed upward by the rapidly rising fireball, which is pushing like a hypervelocity piston.

Figure 2 shows the geometry of an impact just over Jupiter's limb from Earth. Because the dawn terminator is about 7° from the limb, the line-of-sight to the Sun is significantly higher above the point of impact, so that when the luminous fireball rises above the limb, it will not be in the sunlight. If the fireball is moving fast enough (as it will for impacts of 1-km objects), it will continue to rise until it is illuminated by the Sun. This event will be observable if the fireball has cooled and contains enough condensation to scatter the sunlight. If both limb and sunlight times of arrival are determined by observations from Earth, the fireball trajectory can be constructed.

Figure 3 shows fireball trajectories determined by our three-dimensional PCTH simulations for 1- and 3-km impactors, with fireball altitudes plotted as a function of time after impact. Also plotted are line-of-sight elevations from Earth (lightly shaded curves) and the Sun (darker curves) for selected impactors (which are identified by their letter designations). These elevations were determined with the projected impact locations of Chodas and Yeomans. As the impact points rotate toward the limb, the line-of-sight elevations move lower; so these curves decrease with time after impact. This diagram shows how, for a given fragment, (assuming a 1-km or 3-km diameter) the times of arrival over the limb and into the sunlight can be estimated from our calculated trajectories. If these observations are actually made, the true trajectory can be determined. Knowledge of this trajectory, when compared to simulations, will allow the mass of the fragments and their approximate depth of penetration to be determined. These estimates can be further validated by comparing the predicted fireball cooling rate to that determined from time-resolved observations.

Two impacting fragments that are most likely to yield useful data for U.S.-based observers are those labeled R and W, which will both be observable from Hawaii on the final two nights of the series (the R impact may also be observable from the west coast of the United States). Current estimates of the angular distance over Jupiter's limb are 4.7° and 4.0°, respectively. There is some uncertainty associated with these estimates, and they may change by as much as 0.5° by impact time. At the time of impact, the elevation of the direct line-of-sight to Earth will be about 250 and 180 km above the impact points, respectively, assuming that the limb is defined by the cloud tops; high haze could increase this elevation by as much as 40 km. Since R and W are among the brightest fragments, their sizes are considered to be among the largest. From Figure 3 it can be seen that if R and W are 1-km diameter fragments, their fireballs will rise above the limb within tens of seconds of impact, and the debris clouds will enter sunlight within a few minutes. Fragment V will most likely be observable from parts of the continental United States other than the west coast. It will collide on the evening of July 21, but because its impact is just over 6° beyond the limb, it would need to be nearly 3 km in diameter to generate a visible fireball (in which case it would have an apparent magnitude of about 2 as mentioned earlier for a 6° impact). Unfortunately, this fragment appears to be one of the smaller ones, so we are not optimistic. Fragment B is the only other possibility for most continental-U.S. observers, but it is also dim—presumably small—and will impact further over the limb (over 10°) than any other fragment when it hits Jupiter on July 16.

We are enthusiastic about the potential for accomplishing both of our objectives: validation of our simulations and acquiring useful data based on our predictions. Our predictions of observable fireballs are based on the assumption that the impacting fragments are at least kilometer-scale objects. If the fragments are disappointingly small, then our predicted fireballs, along with many of the phenomena anticipated by others, will fail to materialize. In that case, our calculations will

have placed an upper bound of about 1 km on the fragment sizes.

Acknowledgments

This work was supported by the U.S. Department of Energy under contract DE-AC04-94AL85000. This material is based on activities supported by the National Science Foundation under Agreement No. 9322118. Any opinions, findings, and conclusions or recommendations expressed in this publication are those of the authors and do not necessarily reflect the views of the NSF. We are grateful for reviews by Mike Furnish and Marlin Kipp. We thank Paul Chodas for updates on impact times and locations.

References

Boslough, M. B., D. A. Crawford, A. C. Robinson, and T. G. Trucano, Mass and penetration depth of Shoemaker-Levy 9 fragments from time-resolved photometry, *Geophys. Res. Lett.*, in press, 1994.

Crawford, D. A., M. B. Boslough, T. G. Trucano, and A. C. Robinson, The impact of comet Shoemaker-Levy 9 on Jupiter, *Shock Waves*, in press, 1994.

Zahnle, K and M.-M. MacLow, The collision of Jupiter and Comet Shoemaker-Levy-9, *Icarus*, *108*, 1, 1994.

McGlaun, J. M., S. L. Thompson, and M. G. Elrick, CTH: A three dimensional shock-wave physics code, *Int. J. Impact Eng.*, *10*, 351, 1990.

Takata, T., J. D. O'Keefe, T. J. Ahrens, and G. S. Orton, Comet Shoemaker-Levy-9: Impact on Jupiter and plume evolution. *Icarus*, in press, 1994.

Thompson, S. L., ANEOS analytic equations of state for shock physics codes input manual, *SAND89-2951*, Sandia National Laboratories, 1989.

Sound's Effects on Marine Mammals Need Investigation

PAGES 305, 306

Protecting marine mammals and conducting certain types of marine research, in particular, those that use sound in the ocean, have categorically come into conflict because of our lack of knowledge of the effects of low-frequency sound on marine mammals. Despite its intentions to improve Earth's overall environment, the proposed Acoustic Thermometry of Ocean Climate (ATOC) project, and by implication, other uses of sound in the ocean by oceanographers, are now under fire because of the dearth of data on this very issue.

By passing the 1972 Marine Mammal Protection Act, the United States acknowledged that marine mammals are indeed a valuable national resource. Since World War II, the United States has developed and maintained a high-quality marine science research effort.

A National Research Council Ocean Studies Board committee recently presented its research findings on the effects of low-frequency (1–1000 Hz) sound on marine mammals in a report titled "Low-Frequency Sound and Marine Mammals: Current Knowledge and Research Needs."

Although the committee was not instructed to assess the impact of the ATOC experiments and did not focus on those activities in its deliberations, its findings are relevant to the ATOC program.

The committee determined that data on the effects of low-frequency sound on marine mammals are scarce. The bulk of the data is anecdotal, such as, someone heard a sound and some marine mammal behavior was observed, or a specific sound was generated and the observers noted no change in behavior. Few studies correlated the level or intensity of the exposure in the vicinity of the animal with resulting behavior. Without such data, it is impossible to predict the effects of any specific sound exposure.

Moreover, the committee was impeded by a lack of basic knowledge about the hearing of some marine mammals. The question whether they actually hear or detect these very low frequencies largely remains unanswered. For one, researchers do not know the frequency spectrum that whales can hear because there is no real quantitative evidence concerning the range of sound frequencies to which they are sensitive.

For the few marine mammals for which hearing sensitivity data are available, it appears that low-frequency sound, even at very high intensities, is barely audible. Data on the hearing sensitivity of dolphins, small toothed whales, seals, and sea lions suggest that sounds with frequencies below about 100 Hz are practically inaudible to these mammals. But these data, while reasonably consistent, are limited to certain species and cannot be used to evaluate the effects of low-frequency sound on all species of marine mammals.

There are no data available on the auditory sensitivity of any baleen whales or the larger-toothed whales. Overwhelming evidence from several sources suggests that baleen whales are considerably more sensitive to low-frequency sounds than the smaller-toothed whales. In sum, the available data are extremely limited and cannot constitute the basis for informed prediction or evaluation of the long- or short-term effects of intense low-frequency sounds on many marine species. Clearly, more research on marine mammals and their major prey is required. The final section of the report lists several useful research projects.

There are also many sources of sound in the ocean, produced by wind, waves, rainfall, cracking ice, seismic events, and marine organisms, among others, the committee noted. Since the advent of the industrial age, sounds made by human beings have combined with these natural ocean sounds, resulting in elevated noise levels, primarily in the frequency region below 1000 Hz. There are many sources of these sounds; for example, ocean-going vessels, especially large ships such as supertankers, produce high levels.

Other human-made sources include explosive and nonexplosive sounds used in geological exploration for oil and gas; dredging, drilling, and marine construction; surface vessels and submarines; and the sound sources used in oceanographic mapping and research. Sound energy generated by oceanographic experiments is considerably less than that produced by large ships such as supertankers, but again, a precise comparison is impossible because the sound frequencies generated by these sources are different and the sensitivity of marine mammals' hearing at these frequencies is unknown.

Regulations governing the "taking" of marine mammals in research actively discourages and delays the acquisition of scientific knowledge that would benefit conservation of marine mammals, their food sources, and their ecosystems, the committee found. Several alternatives are proposed for reducing unnecessary regulatory barriers and facilitating valuable research, while maintaining necessary protection for marine mammals.

Although the committee strongly agrees with and supports the objective of marine mammal conservation, it believes that the current regulations are unnecessarily cumbersome and restrictive. Not only is research hampered, but the process of training and employing scientists with suitable research skills is impeded.

More humane management of marine mammals depends on better understanding. The present system, in effect, impedes acquisition of the information and understanding needed to pursue a more effective conservation policy.

The 1972 Marine Mammals Protection Act prohibits the "taking" of marine mammals, which has come to be interpreted as any effect ranging from changing the behavior of an animal to killing it. Fisheries have been exempt from this prohibition, although pending legislation may change this. Essentially, there is no regulation of the sound produced by commercial shipping, although their levels are several times higher than those produced by oceanographic experiments.

Ironically, the use of sound for scientific research directed at improving the potential environment of all Earth's inhabitants may be prohibited because it may temporarily disturb some marine mammals, while other activities of no benefit to marine mammals are allowed to kill them.

To sum, the risks of low-frequency sounds to marine mammals are not known. More re-

Fig. 1. Fireball generated by 3-km diameter ice fragment; (a) about 15 s after impact; (b) growing at 50 s, with spherical shock wave forming; (c) at 70 s, with expanding spherical shock. These massively parallel three-dimensional simulations were performed on Sandia's 1840-node Intel Paragon, currently the world's fastest supercomputer.